JOURNAL OF MATERIALS SCIENCE: MATERIALS IN MEDICINE **9** (1998) 583–587

Preparation and mechanical properties of dense polycrystalline hydroxyapatite through freeze-drying

HUI LU, ZHE QU, YANCHUN ZHOU
Institute of Metal Research, Chinese Academy of Sciences, Shenyang 110015, People's Republic of China

High purity hydroxyapatite (HAp) powders were synthesized through the wet-chemical method and subsequent freeze-drying or heat-drying, respectively. Dense polycrystalline HAp ceramics were obtained by sintering the powder compacts in air in the temperature range 1100–1350 °C. Results show that the freeze-drying method can produce highly homogeneous, fine-grained HAp powders. The relative density, Vickers hardness and flexural strength of the sintered freeze-dried HAp ceramics increased with the sintering temperature, reaching a maximum at around 1350 °C, and the highest values obtained were 99.0%, 820 and 110 MPa, respectively. All these mechanical properties of the freeze-dried HAp ceramics are much higher than those of the conventionally heat-dried HAp ceramics. The drying method can significantly influence the properties of the HAp powders as well as the HAp ceramics.

1. Introduction

Dense polycrystalline hydroxyapatite (HAp, $Ca_{10}(PO_4)_6(OH)_2$, Ca/P = 1.667), due to its excellent biocompatibility, has been a particularly attractive material for bone and tooth implants [1–3]. Powder compaction–sintering techniques were often employed to obtain strong forms of HAp ceramics and the HAp powders were usually obtained through the wet-chemical method and subsequent conventional heat-drying [4,5]. However, the heat-dried HAp powders are often in the forms of large agglomerates, and the sintered HAp ceramics are often weak with inhomogeneous pores and thus can hardly meet the requirements for medical application.

Freeze-drying has been shown to be a promising technique for preparing uniform fine-grained powders which can be sintered to very high densities [6,7]. This method has been successful in obtaining homogeneous, fine-grained and highly reactive Al_2O_3 and Fe_2O_3 powders [7,8]. In this work, the wet-chemical method and subsequent freeze-drying was utilized to prepare HAp powders. The obtained HAp powders were then compacted and sintered to obtain the HAp ceramics. The effects of the drying method on the properties of the HAp powders and ceramics were investigated.

2. Experimental procedure

2.1. Material and preparation

Hydroxyapatite powders were prepared by a wet-chemical method and were subsequently freeze-dried. The synthesis procedure for the HAp powders is as follows. (1) 400 ml aqueous solution of 1.75 M $Ca(NO_3)_2 \cdot 4H_2O$ and 300 ml aqueous solution of 1 M $(NH_4)_2HPO_4$ aqueous solution were brought to pH = 10–11 with concentrated NH_4OH (30 vol %). (2) The $Ca(NO_3)_2 \cdot 4H_2O$ solution was vigorously stirred at room temperature, and the $(NH_4)_2HPO_4$ solution was added dropwise over a period of 60 min to the calcium solution. (3) The reaction mixture was heated to 90 °C and kept for 24 h with stirring, and was then filtered three times with distilled water to obtain a sticky mixture of precipitate and water.

The filtered mixture of precipitate and water was then freeze-dried on a home-made freeze-drying apparatus [9]. The freeze-drying process was as follows. The sticky precipitate was rapidly frozen by mixing with liquid nitrogen, then the frozen mixture was put into the cold room of the freeze-drying apparatus to which a vaccum pump is attached. The cold room was then kept at a low pressure of about 3–6 bar (1bar = 10^5 Pa) by the vacuum pump to let the frozen water sublime. A compressor was used to keep the room at a temperature around 0 °C to make sure that the frozen mixture did not melt during the freeze-drying process. The freeze-drying process was accelerated by an infrared lamp at an intensity of about 3000 $W\,m^{-2}$ at a later stage. The samples were freeze-dried for 36–70 h before they were removed from the apparatus. For the purpose of comparison, part of the filtered sticky mixture was also heat-dried at 105 °C for 48 h and then ball-milled to obtain the heat-dried HAp powders.

The freeze-dried HAp (FD-HAp) and the heat-dried HAp powders (HD-HAp) were calcined at 800 °C for

3 h, then premoulded and hydrostatically pressed at 200 MPa into rectangular-shaped compacts with the size of $50 \times 4 \times 5\ \mathrm{mm}^3$. The green compacts of HAp were sintered in air for 3 h in the temperature range 1100–1350 °C, and were cooled to room temperature in the furnace.

2.2. Sample characterization

Samples were characterized at room temperature. After calcining, the HD-HAp powders were ball-milled again, while the HD-HAp powders were left as they were. The Ca/P atomic ratio of the calcined HAp powders was measured by chemical analysis. Small amounts of calcined FD-HAp and HD-HAp powders were dispersed by ultrasonic waves in alcohol for 120 s, and then deposited on a copper grid for transmission electron microscopic (TEM, Philips EM420) observation.

The sintered FD-HAp and HD-HAp samples were ground with 800-grit SiC (emery) paper to a precise rectangular shape. The density of the samples was measured by the fluid-displacement method with distilled water on a densitometer (Satorious YDK01) with an accuracy of $\pm 0.1\%$. Vickers hardness was measured at a load of 50 g, and each sample was indented seven times to obtain the statistical average hardness values. Flexural strength (three-point bending strength) of the sintered HAp samples was measured on a Shimadzu Testing Machine (EHF-FB01-4LA) at a loading rate of $1.25\ \mathrm{mm\,min^{-1}}$. The fracture surfaces of both the FD-HAp and HD-HAp ceramics sintered at different temperatures were etched with citric acid (0.15 M) for 10 min, and were then examined using a scanning electron microscope (SEM, Cambridge S360). An X-ray diffractometer (XRD, Rigaku D/max-rA) was used to characterize the two types of HAp powders and compacts.

3. Results and discussion

3.1. Characterization of the HAp powders

The Ca/P ratio of the HAp powder is one of the most crucial parameters in determining the properties of the HAp [10]. Chemical analysis results are presented in Table I, it is clear that both the Ca/P ratio and the calcium and phosphorus elemental contents for the calcined freeze-dried HAp powder (FD-HAp) coincide well with the theoretical values for pure HAp. Those for the calcined heat-dried HAp (HD-HAp) powders are actually the same as that of the FD-HAp powders. It is worth noting that there was always a deficiency in weight percentage of calcium and phosphate in synthesized HAp, although the Ca/P ratio may be close to the ideal stoichiometry [1]. The XRD pattern of the calcined FD-HAp powders is shown in Fig. 1a, from which we can see that all the diffraction peaks are those for the crystalline HAp, indicating that no detectable impurity exists in the HAp powders.

TABLE I Results of chemical analyses for HAp powders after calcining at 800 °C for 3 h

HAp samples	Ca (wt %)	P (wt %)	Ca/P (mol)
Pure HAp	39.90	18.50	1.667
Jarcho *et al.* [1]	37.4	17.1	1.69
Jarcho *et al.* [1]	36.6	17.1	1.65
Present work	39.3	18.1	1.67

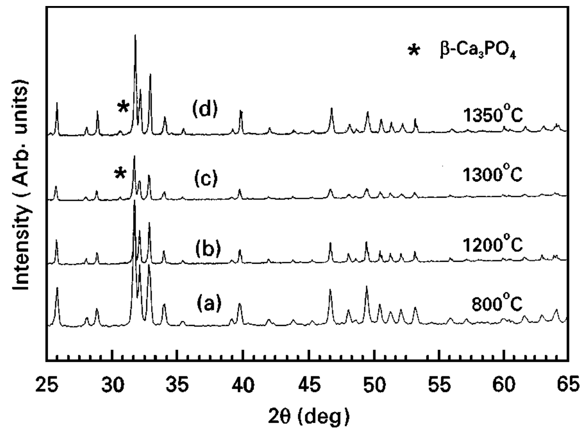

Figure 1 X-ray diffraction patterns for FD-HAp, (a) FD-HAp powder calcined at 800 °C for 3 h; and FD-HAp ceramics sintered at (b) 1200 °C, (c) 1300 °C and (d) 1350 °C for 3h.

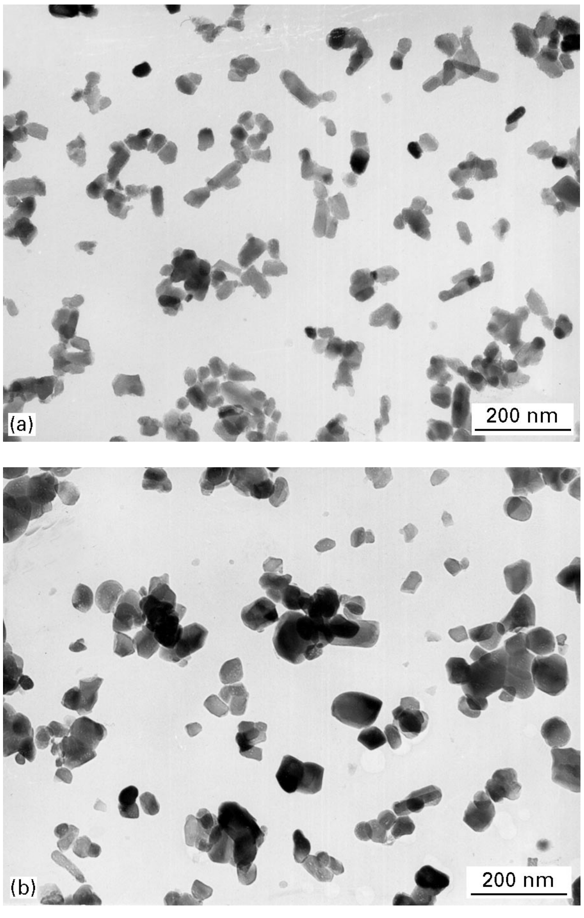

Figure 2 Transmission electron micrographs of HAp powders after calcining at 800 °C for 3 h: (a) FD-HAp, (b) HD-HAp.

TEM images of the calcined FD-HAp and HD-HAp powders are shown in Fig. 2a and b, respectively. It is clear that the mean crystallite size of the FD-HAp powder is smaller than that of the HD-HAp powders; the FD-HAp powders are homogeneous, while the

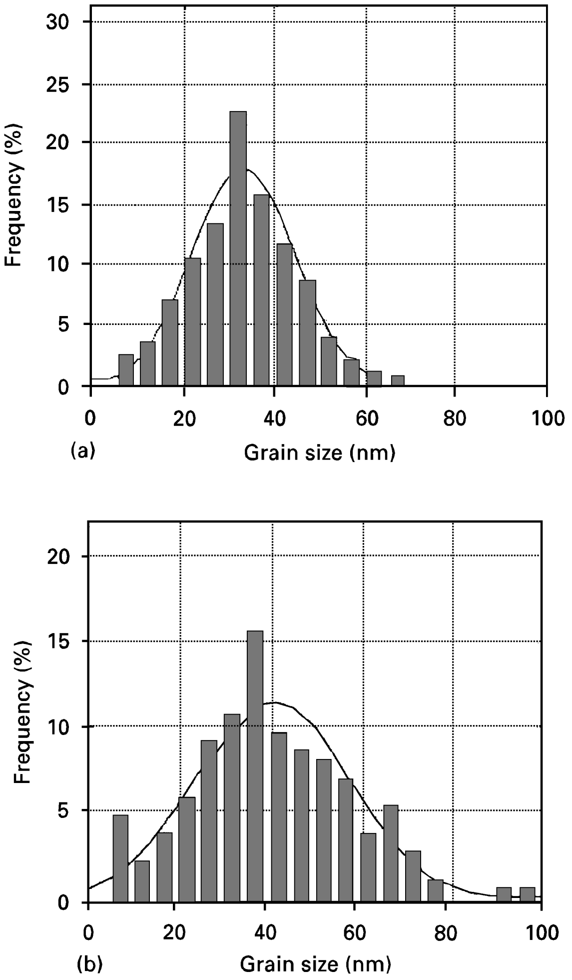

Figure 3 Grain-size distribution for the HAp powders: (a) FD-HAp, (b) HD-HAp.

HD-HAp powder is often in the form of large agglomerates. The grain-size distribution for the two types of HAp powders (Fig. 3) was taken by direct computer-based image analysis on the TEM images in Fig. 2. The grain-size range of the FD-HAp powders (Fig. 3a) is evidently narrower than that of the HD-HAp powders (Fig. 3b), and the mean grain size for the FD-HAp powders is about 33 nm, while that of the HD-HAp powders is about 40 nm. It is clear that the freeze-drying method can produce fine-grained, homogeneous HAp powders.

3.2. Characterization and properties of the HAp ceramics

3.2.1. X-ray diffraction

Fig. 1b–d show the XRD patterns of the FD-HAp compacts sintered for 3 h in air at 1200, 1300 and 1350 °C, respectively. It is clear that all the diffraction peaks of the HAp ceramics sintered at 1200 °C are those of the HAp phase, with no extraneous phase, while an additional weak diffraction peak due to β-$Ca_3(PO_4)_2$ ($2\theta = 30.03°$) was observed in the XRD pattern of the 1300 °C sintered FD-HAp compacts (Fig. 1c). Therefore, it can be concluded that the decomposition temperature of the FD-HAp is somewhere between 1200 and 1300 °C, and that the FD-HAp decomposes into the β-$Ca_3(PO_4)_2$ phase. After sintering at 1350 °C, the diffraction peak for the second β-$Ca_3(PO_4)_2$ phase is still very weak, indicating that the decomposition rate of the FD-HAp is very low, even at 1350 °C. The high thermal stability of the HAp samples may be correlated with the perfect Ca/P ratio of the HAp. The high thermal stability of the HAp is very important in practical applications of the HAp materials, as a high thermal stability is often a prerequisite for the sinterability of the HAp. For example, a low thermal stability of the HAp may be pernicious, as the HAp may decompose into β-$Ca_3(PO_4)_2$, α-$Ca_3(PO_4)_2$, and/or $Ca_2P_2O_9$ at temperatures well below their sintering temperature, thus retarding the densification process of the HAp compacts [4, 11].

XRD results show that HD-HAp compacts sintered under the same condition as that of FD-HAp exhibit similar XRD diffraction patterns as indicated in Fig. 1. The FD-HAp and HD-HAp samples have similar thermal stability and very close Ca/P ratio, but a difference exists in the morphology of the two kinds of HAp powders.

3.2.2. Densification and microstructure

The variation in density with sintering temperature for the FD-HAp and HD-HAp blocks is shown in Fig. 4. The density of the two types of HAp blocks increased with the sintering temperature, and the attained density of FD-HAp is often higher than that of HD-HAp. When the sintering temperature was higher than 1200 °C, the density versus sintering temperature curve for the HD-HAp was rather flat, while the density of the FD-HAp blocks increased steadily with the increasing sintering temperature. After sintering at 1350 °C, the relative densities for FD-HAp and HD-HAp blocks reach a maximum, being 99.0% and 96.7%, respectively (the theoretical density for hydroxyapatite is 3.156 $g\,cm^{-3}$).

The most translucent and densified FD-HAp samples were obtained after sintering at 1350 °C; a typical scanning electron micrograph of these 1350 °C sintered FD-HAp samples is presented in Fig. 5a, which showed very few pores in the micrograph and

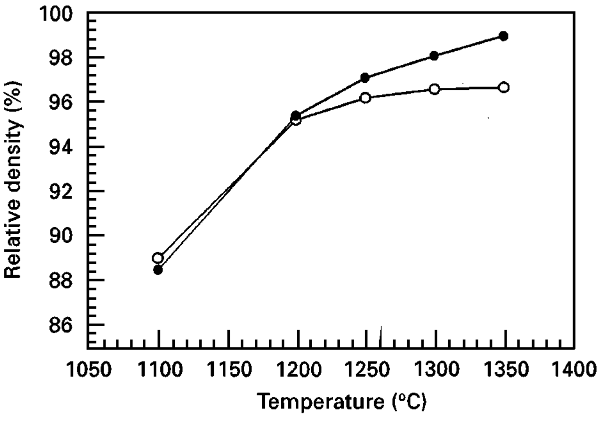

Figure 4 Relative density of the HAp ceramics as function of sintering temperatures: (●) FD-HAp, (○) HD-HAp.

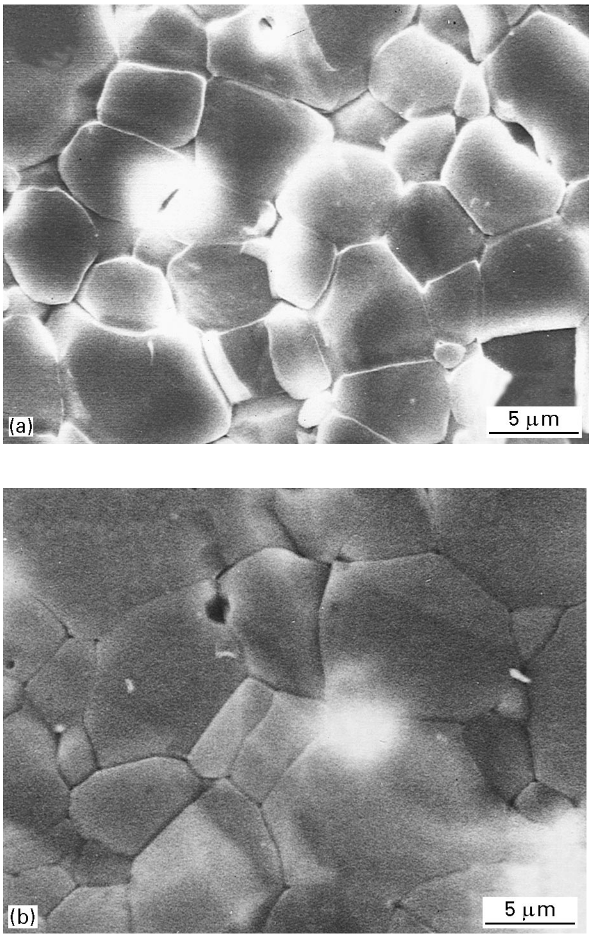

Figure 5 Scanning electron micrographs of etched fracture surfaces of (a) the FD-HAp, and (b) the HD-HAp, sintered for 3 h at 1350 °C.

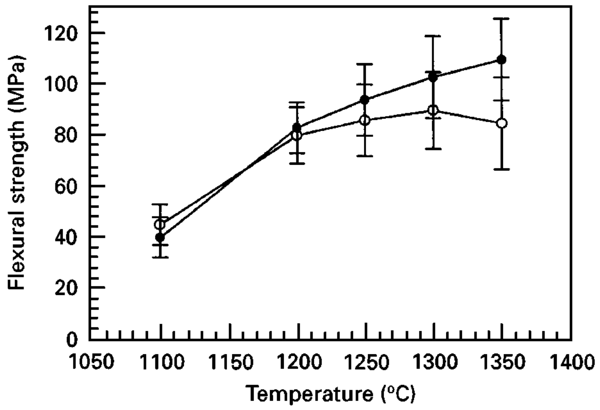

Figure 6 Flexural strength of the HAp ceramics as a function of sintering temperatures: (●) FD-HAp, (○) HD-HAp.

the grain sizes were rather uniform. A scanning electron micrograph of the HD-HAp samples after sintering at 1350 °C is shown in Fig. 5b; there is marked evidence of exaggerated grain growth after sintering at 1350 °C, which could be due to the agglomerated precursor HD-HAp powders, as shown in Fig. 2.

3.2.3. Flexural strength

The measured flexural strength of the two types of HAp compacts is shown in Fig. 6 as a function of the sintering temperature. The flexural strength of the sintered FD-HAp bars increases with sintering temperature until it reaches the maximum value of 110 MPa at 1350 °C, while that of the HD-HAp bars reaches a maximum value of 90 MPa at 1300 °C and then decreases slightly at the sintering temperature of 1350 °C. The slight drop in the flexural strength of the HAp may be due to the abnormal grain growth in the HD-HAp, as can be seen in Fig. 5b.

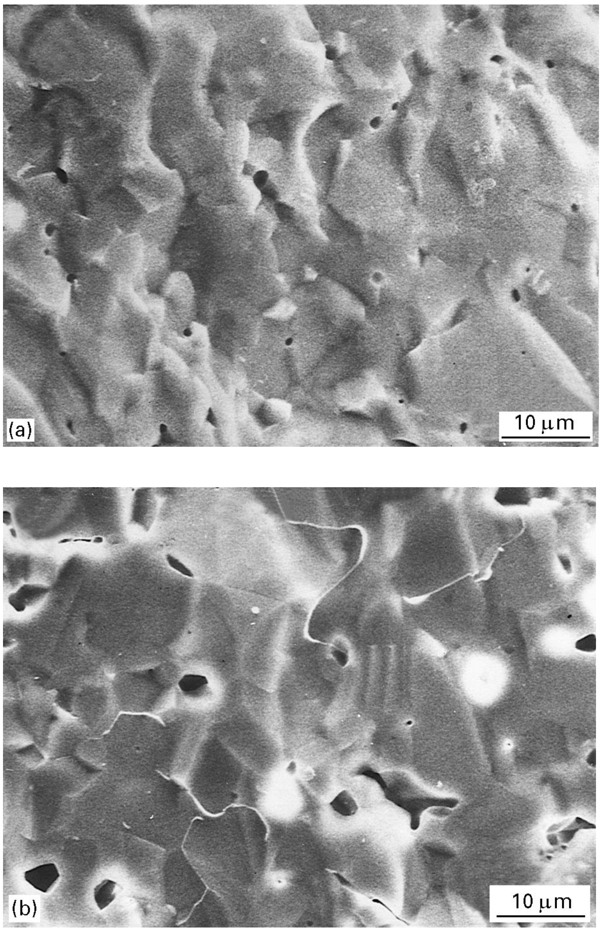

Figure 7 SEM morphologies of the fracture surfaces of (a) FD-HAp and (b) HD-HAp sintered at 1350 °C for 3 h.

SEM examination of the fracture surfaces (Fig. 7) produced by flexural tests revealed interesting information concerning the nature of fracture. The HD-HAp bars sintered in air for 3 h at 1350 °C failed by a characteristic transgranular fracture process (Fig. 7b). The FD-HAp bars sintered under the same conditions exhibited a mainly transgranular fracture, but some intergranular fracture can also be observed around the grain-boundary pores (Fig. 7a).

3.2.4. Vickers hardness

The variation in the Vickers hardness of the two types of HAp compacts with sintering temperature (Fig. 8) is similar to that of the density, it increases with the increment of the sintering temperature, implying that hardness is controlled by the bonding between the particles in the sintered compacts. Like the density, Vickers hardness of FD-HAp compacts is always higher than the corresponding values for HD-HAp

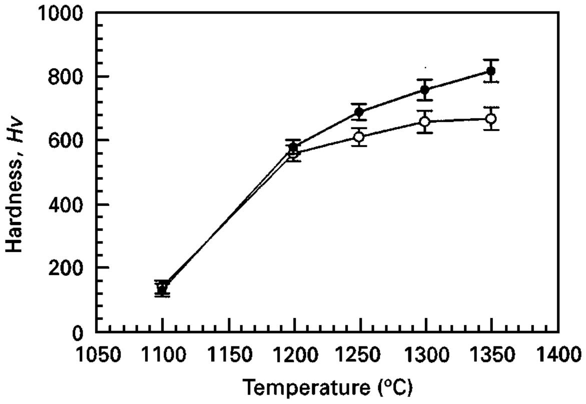

Figure 8 Vickers hardness of the HAp ceramics as a function of sintering temperatures: (●) FD-HAp, (○) HD-HAp.

compacts. The maximum hardness for the FD-HAp samples amounts to 820 MPa, compared to 670 MPa for the HD-HAp. The obtained Vickers hardness of the FD-HAp samples amounts to 820 MPa, which is much higher than the values reported in the literature [4, 5, 12, 13], of which the Vickers hardness values are somewhere in the range of 480–620 MPa.

A high hardness is the guarantee for a good wear resistance, which is crucial for HAp materials which are often applied in tooth and bone implantation. Many factors may affect the hardness of HAp materials, for example, the density, Ca/P ratio, possibly the weight percentage of the Ca^{2+}, and so on. It is interesting to note that the weight percentage of calcium is much higher than the values reported elsewhere [1], as indicated in Table I. The high Vickers hardness of HAp may be due to the high calcium weight percentage in FD-HAp samples. Further work is needed to identify the relationship between the hardness and weight percentage of the Ca^{2+}. However, it should be noted that the load we used to measure the hardness is comparatively lower than those used in the literature, which might lead to a slightly higher Vickers hardness value.

The two kinds of HAp compact, which were prepared through nearly identical synthesis routes except the drying method, maintain distinctly different densification rate and mechanical properties. The sintered FD-HAp compacts are much denser and their mechanical properties are superior to those of sintered HD-HAp compacts. These differences between the two types of HAp compacts can then be reasonably attributed to the difference in the precursor powders, which were dried through different methods, i.e. the freeze-drying and the conventional heat-drying methods. As shown in the micrographs, the FD-HAp powders are fine-grained and homogeneous, and thus its compacts can be sintered to a much higher density than the HD-HAp powders. Furthermore, the freeze-dried HAp powders do not require a subsequent ball-milling process, thus avoiding sample contamination and air pollution. The freeze-drying method is promising in synthesizing dense polycrystalline HAp.

4. Conclusion

The freeze-dried HAp powders are fine grained, homogeneous, and maintain a high thermal stability. The sintered FD-HAp compacts have much higher density, flexural strength, and hardness than the corresponding values for the HD-HAp compacts. The relative density for the 1350 °C sintered FD-HAp is 99.0%, and the flexural strength and Vickers hardness are 110 and 820 MPa, respectively.

Acknowledgement

The Chinese Academy of Sciences is gratefully acknowledged for the financial support of this work.

References

1. M. JARCHO, C. H. BOLEN, M. B. THOMAS and R. H. DOREMUS, *J. Mater. Sci.* **11** (1976) 2020.
2. K. DE GROOT in "Bioceramics of Calcium Phosphate", edited by K. de Groot (CRC Press, Boca Raton, FL, 1983) p. 99.
3. L. L. HENCH, *J. Am. Ceram. Soc.* **74** (1991) 1487.
4. P. E. WANG and T. K. CHAKI, *J. Mater. Sci. Mater. Med.* **4** (1993) 150.
5. T. KIJIMA and M. TSUTSUMI, *J. Am. Ceram. Soc.* **62** (1979) 455.
6. D. B. HIBBERT and A.C.C. TSEUNG, *J. Mater. Sci.* **14** (1979) 2665.
7. L. A. BEYER, C. E. KALNAS, D. B. ROY and I. K. LLOYD, *Am. Ceram. Soc. Bull.* **66** (1987) 1647.
8. D. W. JOHNSON and F. J. SCHNETTLER, *J. Am. Ceram. Soc.* **53** (1970) 440.
9. H. LU, Master Thesis, Institute of Metal Research, Chinese Academy of Sciences (1996).
10. R. ROYER, J. C. VIGUIE and M. HEUGHEBAERT, *J. Mater. Sci. Mater. Med.* **4** (1993) 76.
11. J. ARENDS and J. CHRISTOFFERSEN, *J. Cryst. Growth* **84** (1987) 515.
12. P. VAN LANDUYT, F. LI, F. DELANNAY and E. MUNTING, *J. Mater. Sci. Mater. Med.* **6** (1995) 8.
13. M. AKAO, H. AOKI and K. KATO, *J. Mater. Sci.* **16** (1981) 809.

Received 29 April
and accepted 25 September 1997